GRANULAR OPEN FILTERS ON A HORIZONTAL BED UNDER WAVE AND CURRENT LOADING

Guido Wolters¹ and Marcel R.A. van Gent²

Rubble mound coastal structures typically contain granular filters in one or more layers. These filters are normally geometrically tight (to prevent material washout), often difficult to realize in the field, and expensive. An alternative is a geometrically open filter (*i.e.* a large ratio of the size of toplayer material and underlayer material), designed in such a way that it fulfills its filter functions with only minimal base material loss or settlement. Potential applications of open filters under wave and current loading could lead to significant cost and material savings, and to a more practical application of filters in the field. The physical model tests conducted in this study focus on granular open filters on a horizontal sand bed under wave and combined wave & current loading.

Keywords: rubble-mound breakwater; open filter; transport filter; waves; currents; physical model tests

INTRODUCTION

The majority of rubble mound coastal structures contains granular filters where a large rock grading is positioned on top of a smaller rock grading, often with one or more layers. These filters are normally geometrically tight filters (no material washout). Underneath the filter layers quarry material is present, or a combination of a geotextile with sand as core material.

Geometrically tight filters are often difficult to realize and expensive. In many instances a large number of filter layers and material volume is required. Furthermore, geometrically tight filters are often difficult to realise in the field because of quarry material limitations and when the structure is constructed underwater.

An alternative is a geometrically open filter (*i.e.* a large ratio of the size of toplayer material and underlayer material). In this case the filter is designed in such a way that the hydraulic loading is too low to initiate erosion of base material (or settlement) outside an acceptable range. Limited settlement is often permitted in the field. Potential applications of open filters include bed protections and toe & slope configurations of coastal structures. The allowed settlement depends on the structure type. For breakwaters and revetments even small amounts of toe settlement can endanger the stability of the armour layer by loosening the bonds between interlocked armour units or placed block revetments. This could lead to the failure of the structure as a whole (see *e.g.* CIRIA, CUR, CETMEF 2007).

Geometrically open filters are either hydraulically closed filters (in which incipient motion of base material is not exceeded) or transport filters (in which transport of base material occurs). Transport filters can be subdivided into filters where transport of base material occurs only within the filter and filters where base material transport occurs also outside the filter.

Proper guidelines on the design of geometrically open filters that allow an acceptable and predictable loss of base material under wave and current loading, could lead to significant cost and material savings, and to a more practical application of filters in the field.

The presented work is an exploratory study for a more extended research effort on open filters. The physical model tests that are described here focus on granular open filters on a horizontal sand bed under wave and combined wave-current loading.

PREVIOUS RESEARCH

In the 1980s and 1990s a large number of tests have been performed by *e.g.* De Graauw *et al* (1983), Bakker *et al* (1994), Klein Breteler (1989), Klein Breteler *et al* (1992) to determine criteria for the initiation of motion in granular filters. This research has resulted in various formulae and design diagrams for interface stability of granular filters, which have been incorporated in CUR report 161 (1993). Furthermore, new criteria for interface stability have been introduced in CUR report 233 (2010), which are however not yet verified by experimental data.

¹ Deltares, P.O. Box 177, 2600 MH, Delft, The Netherlands, guido.wolters@deltares.nl

² Deltares, P.O. Box 177, 2600 MH, Delft, The Netherlands, marcel.vangent@deltares.nl

The above mentioned research studies have been conducted with a focus on steady flow and the initiation of base material transport through/within the filter. The studies do not specifically address base material transport itself or filter settling effects.

Very little knowledge is available about base material transport (and critical hydraulic gradients) in filters under cyclic (unsteady) loading. Reference is made to De Graauw *et al* (1983), who focussed on cyclic flow perpendicular to the sand-filter interface, Uelman (2006) and Ockeloen (2007), who studied a breakwater with an open filter but did not develop a criterion for the assessment of incipient motion under wave loading and Dixen *et al* (2008), who determined the onset of transport of sand underneath single sized armour blocks. Although these studies discuss various aspects of cyclic (wave) loading, they do not specifically address the problem of base material transport in filters.

To design open filters for applications under wave loading, and combined wave-current loading, more information is needed before the potential cost-savings of applying open filters can be scientifically justified. Therefore, the present study focusses on granular open filters on a sand bed under wave and combined wave & current loading.



Figure 1. Wave flume: Breaking waves above open filter.

In the following section the criteria for the initiation of motion in granular filters (steady flow), as presented by De Graauw *et al* (1983), Klein Breteler (1989), Klein Breteler *et al* (1992) are discussed in more detail.

Critical filter velocity & critical hydraulic gradient

In his study from 1989, Klein Breteler (1989) analyses a horizontal, steady flow through a granular filter on top of a sand bed. Sand transport measurements were conducted from which the critical filter velocity and critical gradient at the beginning of transport were determined. Based on the measurements Klein Breteler (1989) and Den Adel (1992) derived Equations 1 and 2 for the critical filter velocity, $u_{f,cr}$, for the initiation of base particle motion under steady flow:

$$u_{f,cr} = \left[\frac{n_f}{c} \left[\frac{D_{15,f}}{v_w}\right]^m \sqrt{\psi \cdot g \cdot \Delta \cdot D_{50,b}}\right]^{1/(1-m)} \quad \text{for } 0,1 \text{ mm} < D_{50,b} < 1 \text{ mm}$$
(1)
$$u_{f,cr} = \frac{n_f}{0.22} \sqrt{\left(\psi \cdot g \cdot \Delta \cdot D_{50,b}\right)} \quad \text{for } D_{50,b} > 0,7 \text{ mm}$$
(2)

with

- $u_{f,cr}$ = critical filter velocity, where u_f is the averaged velocity over the cross-section of the filter (m/s)
- g = acceleration due to gravity (m/s²)
- $\Delta = \rho_s / \rho_w 1$ = relative submerged density of base material (-)
- ρ_s = density of base material, ρ_w = density of water (kg/m³)
- Ψ = Shields parameter for base material (-).
- m,c = constants, dependent on $D_{50,b}$ (-); see Table 1.
- v_w = kinematic viscosity of water (m²/s)

$D_{b50} ({ m mm})$	c (-)	m (-)	
0,1	1,18	0,25	
0,15	0,78	0,20	
0,2	0,71	0,18	
0,3	0,56	0,15	
0,4	0,45	0,11	
0,5	0,35	0,07	
0,6	0,29	0,04	
0,7	0,22	0	
0,8	0,22	0	
1,0	0,22	0	

For the critical hydraulic gradient (parallel to the filter-bed interface, as measured in this study) the following empirical relationship can be used, developed for initiation of transport under steady flow (De Graauw, 1983), see Equation 3:

$$i_{cr} = \left[\frac{0.06}{n_f^3 D_{15,f}^{4/3}} + \frac{n_f^{5/3} D_{15,f}^{1/3}}{1000 D_{50,b}^{5/3}}\right] u_{*cr}^2$$
(3)

where (for sand as base material, Equation 4):

$$u_{*cr} = 1.3D_{50,b}^{0.57} + 8.3 \cdot 10^{-8} D_{50,b}^{-1.2}$$
⁽⁴⁾

with

 $D_{15,f}$ = diameter of filter material exceeded by 85% (mass) (m)

 $D_{50,b}$ = diameter of bed material exceeded by 50% (mass) (m)

 i_{cr} = critical hydraulic gradient, parallel to the filter-bed interface (-)

 u_{*cr} = critical shear velocity of base material (m/s)

 n_f = porosity of filter material (-)

Please note that Equations 3 and 4 are dimension-dependent. Very similar results to Equation 3 are obtained if i_{cr} is calculated using the Forchheimer equation (based on u_{cr}). Furthermore, experience (at prototype) has shown that the De Graauw criteria is relatively conservative. The Forchheimer equation could lead here to larger i_{cr} values (and thus to smaller required filter layers). For more information on the Forchheimer relation as applied to granular filters, reference is made to CUR 161 (1993) and Van Gent (1995).

Based on the previously introduced formula for the critical filter velocity and the critical hydraulic gradient the following critical values can be calculated for $D_{f,15} = 20\text{-}30\text{mm}$ (stationary current): $u_{f,cr} \approx 0.02\text{-}0.03 \text{ m/s}$ and $i_{cr} \approx 0.06\text{-}0.07$.

The current study indicates that (as Klein Breteler *et al* surmise in their 1992 study) the above described criteria for initiation of motion are also applicable to cyclic loading. Initiation of motion was observed for $i/i_{cr} \sim 1$. These initial tests are not described in this paper, since they did not result in any base material transport (see section on observations).

Macroscopic transport model

Based on the critical hydraulic gradient (respectively the critical filter velocity), as introduced in the previous section, Klein Breteler *et al* (1992) developed the following empirical transport formulae for macroscopic base material transport within filters (steady flow, homogeneous base material):

$$T = \rho_s \cdot p_1 \cdot \left(i / i_{cr} - 1 \right)^{1.25}$$
(5)

$$T = \rho_s \cdot p_2 \cdot \left(\left(u_f / u_{f,cr} \right)^2 - 1 \right)^{1.5}$$
(6)

where:

T = transport rate in (kg/m/s) $\rho_s = \text{density of transported material (kg/m³)}$ $u_{f,cr} = \text{critical filter velocity (m/s)}$ $i_{cr} = \text{critical hydraulic gradient, parallel to the filter-bed interface (-)}$ $p_i = \text{transport intensity (m³/m/s)}$

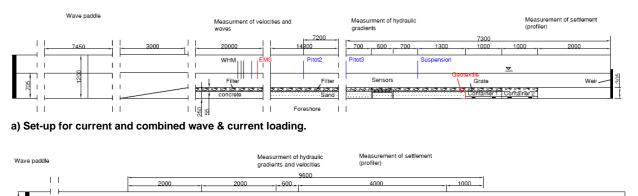
These formulae are based on the assumption of a turbulent flow, *i.e.* the hydraulic gradient is proportional to the square of the filter velocity. Equation 6, based on $u_{f,cr}$, was derived from the classical formula of Meyer-Peter and Mueller for bedload transport in free surface flows.

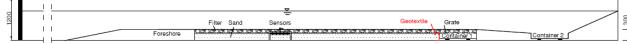
The value of the transport intensity, p_i , was found to be independent of the diameter of the transported material and in the range of:

$$p_i = 0.6 \ge 10^{-6} - 9.0 \ge 10^{-6} \text{ m}^2/\text{s}$$
 with a best fit for $p_i = 1.5 \ge 10^{-6} \text{ m}^2/\text{s}$

PHYSICAL MODEL TESTS

Physical model tests were performed in a wave & current flume (length 110m, width 1m, height 1.2m) at Deltares, Delft. The set-up of the model consisted of a submerged granular filter construction on a sand bed which was subjected to waves, currents and wave & current loading, see Figure 2.





b) Set-up for wave loading (see Wolters et al, 2010).

Figure 2. Model set-up in the Scheldt Flume of Deltares, Delft.

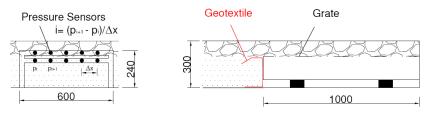


Figure 3. Pressure transducer frame at rock-sand interface (2 rows of 5 pressure sensors each, 25mm above and below the filter-sand interface).

A concrete foreshore (0.305m thick) was used in which a granular filter layer of $d_f = 0.055$ m or 0.1m thickness ($D_{n50,f} = 20$ -30mm, $d_{f}/D_{n50,f} = 1.8$ -3.3, $M_{85,f}/M_{15,f} = 3.4$ -4.6, $\rho_{s,f} = 2650$ -2700 kg/m³) and a sand layer of $d_b=0.25$ m or 0.205m thickness ($D_{50,b}=0.15$ -0.16mm, $D_{50,f}/D_{50,b}=150$ -220) were embedded. Tests were conducted for two filter thicknesses (plus a reference case without filter) and two filter stone sizes. The porosity of the filter material was estimated from the sieving curve to be n = 0.44. The horizontal concrete-filter section (length L = 20m) in front of the measurement area allowed

the turbulent flow conditions within the filter layer and the full water depth to become fully developed before any measurements were conducted. The transported sand was collected in two containers behind the filter section.

Measurements were performed of the incident waves, velocities above the filter bed, base material (sand) transport, filter settlement using a mechanical profiler, pressures and pressure gradients in filter and sand bottom (*e.g.* Figure 2 and 3). Also instrumentation was present to measure the water surface and the velocity profile. Ripple lengths, heights and sand movements along the seabed were also monitored. The hydraulic gradients i and i_{cr} have been directly measured at the sand-filter interface (parallel to interface). A wide grading of the filter material was chosen since these are the most realistic to be applied in open filters.

Waves up to $H_s = 0.2m$ (JONSWAP spectrum, second-order waves) were generated and horizontal depth-averaged current velocities up to $u_m = 1.25$ m/s. The base material (sand) and the water depth above the open filter ($h_f = 0.4m$) were kept constant during all tests. Conditions in the filter bed were always in the turbulent regime (though fully turbulent conditions were not always achieved).

 KC_f numbers between $KC_f = (u_{2\%}T_m)/(n_fd_f) = 10 - 250$ (based on $u_{2\%}$ = velocity directly above the filter exceeded by 2% of waves), and mobility numbers between $\theta_{max} = u_{max}^2/g/\Delta/D_{50,b} = 49 - 1388$ ($\theta_{2\%}$ = 27 - 794) were measured. The KC_f number is here based on the filter thickness d_f instead of the filter stone diameter $D_{n50,f}$.

Test	Loading	Test parameters			Loading conditions				Measured			
	-	D _{n50 f} d _f	•	h _f	Hs	T _p	Sop	um	t _{Tot}	u _{2%}	Т	T*
		(mm)	(m)	(m)	(m)	(s)	(-)		(hrs)	(m/s)	(g/m/s)	(-)
T01	current	22	0,055	0,4	-	-	-	1,25	8,48	1,00	0,062	0,0029
T02	current + waves	22	0,055	0,4	0.06	1,98	0,009	0,63	0,50	0,68		
T03	current + waves	22	0,055	0,4	0,11	2,51	0,011	0,13	6,00	0,35	0,008	0,0004
T04	current + waves	22	0,055	0,4	0,15	3,01	0,011	0,13	6,00	0,71	0,007	0,0003
T05	current + waves	22	0,055	0,4	0,12	2,99	0,008	0,63	6,00	1,03	0,031	0,0014
T06	current + waves	22	0,055	0,4	0,12	5,08	0,003	0,63	6,00	0,92	0,043	0,0020
T07	current + waves	22	0,055	0,4	0,14	5,69	0,003	0,63	6,00	1,14	0,063	0,0029
T08	current	22	0,055	0,4	-	-	-	1,06	6,00	1,02	0,052	0,0024
T09	current + waves	22	0,055	0,4	0,10	5,07	0,002	1,06	4,18	1,43	0,203	0,0094
T10	current	22	0,055	0,4	-	-	-	0,63	6,00	0,60	0,006	0,0003
T11	current	22	0,055	0,4	-	-	-	1,06	6,00	0,91	-	-
T12	current + waves	22	0,055	0,4	0,10	5,08	0,002	1,06	2,00	1,20	0,331	0,0153
eference tests	(without filter)											
T13	current	-	-	0,455	-	-	-	0,55	0,50	0,65	12,265	0,5684
T14	current + waves	-	-	0,455	0,13	5,10	0,003	0,55	0,50	1,13	33,553	1,5550
Vave tests (Wo	ters et al. 2010)											
T05	waves	30	0,1	0,4	0,10	2,09	0,015	-	6	0,26	0,102	0,0047
T06	waves	30	0,1	0,4	0,14	2,52	0,014	-	6	0,38	0,079	0,0037
T07	waves	30	0,1	0,4	0,17	5,41	0,004	-	2	0,88	0,161	0,0075
T08	waves	30	0,055	0,4	0,14	2,52	0,014	-	6	0,43	0,063	0,0029
T09	waves	30	0,055	0,4	0,14	1,80	0,027	-	6	0,32	0,063	0,0029
T10	waves	30	0,055	0,4	0,16	5,10	0,004	-	2	0,86	0,068	0,0031
T11	waves	20	0,055	0,4	0,14	2,52	0,014	-	6	0,41	0,035	0,0016
T12	waves	20	0,055	0,4	0,14	1,81	0,027	-	6	0,32	0,033	0,0015
T13	waves	20	0,055	0,4	0,16	5,10	0,004	-	2	0,88	0,040	0,0019

The test programme is given in Table 2. The test duration (t_{Tot}) varied between tests, based on the observed base material transport (1000-12000 waves). Short duration tests (1000 waves) were employed for the reference case without filter layer, due to the large amounts of sand transported. The measured transported base material is given in Table 2 as T(g/m/s) and in dimensionless form T^* (-):

$$T^* = \frac{T / \rho_s}{\sqrt{\Delta g D_{50,b}^3}} \tag{7}$$

where:

 Δ = relative buoyant density of base material ($\rho_s / \rho_w - 1$)

OBSERVATIONS

Wave loading (see Wolters et al, 2010)

The tests were originally set-up to investigate bedload and suspended load transport separately. However, it became apparent during testing that these two regimes could not be separated, since significant base material transport could only be realized once the filter velocities were far above the critical velocity and once base material was also suspended in the water column. Measurable material transport was first observed for wave heights of $H_s = 0.1$ m and $u_{2\%} = 0.25$ m/s ($i_{2\%}/i_{cr} = 2$, $u_{2\%}/u_{cr} = 10$ -14). At this stage bed ripples beneath the filter layer became fully formed with heights of 10-20 mm and 70-170 mm length.

The observed base material transport for wave loading alone was very low (T < 0.16 g/s/m) for all tested filter configurations, even for large near-bed velocities ($u_{2\%}/u_{cr} = 10-38$) and hydraulic gradients ($i_{2\%}/i_{cr} = 2-3.7$), see Figure 6. It was observed that while the hydraulic gradients (measured parallel to the filter-bed interface) were sufficiently high to produce initiation of motion around the rest position and some suspension of bed material, most of the bed material remained in its original vicinity.

The tests showed that the base material distribution (sieving curve) changed during transport. Whereas the original sand (current loading) had a median particle size of $D_{50,b} = 152 \,\mu\text{m}$, the particle size of the transported bedload material was $D_{50,b} = 142 \,\mu\text{m}$ and that of the suspended load $D_{50,b} = 104 \,\mu\text{m}$. The heaviest sand particles were left behind during bedload transport and only the lighter particles were transported in suspended mode. It was observed that the finer sand particles were entrained into the water column (particles < 60 μm) very quickly, clouding the water. Most of this material was so fine that it remained suspended in the water column even days after testing.

Current loading

For low current velocities ($u_{2\%} < 0.6 \text{ m/s}$) no base material transport was observed. Measurable material transport was observed at $u_{2\%} > 1 \text{ m/s}$ ($i_{2\%}/i_{cr} > 2$, $u_{2\%}/u_{cr} > 19$). First particle clouds were seen moving through the filter, and initial scouring at some stone locations occurred.

Compared to the case of wave loading the velocity at (observed) transport initiation was somewhat larger ($u_{2\%}/u_{cr} = 19$ in place of $u_{2\%}/u_{cr} = 10$ -14), although the hydraulic gradient was similar ($i_{2\%}/i_{cr} \approx 2$).

The observed base material transport for current loading was very low (<0.06 g/s/m) for all tested filter configurations, see Figure 5.

Wave & current loading

$U_{2\%} < 0.6 \ m/s \ (i_{2\%}/i_{cr} < 2.3)$

First entrainment of small sand clouds into the filter was observed at $H_s = 0.11$ m, but the observed base material transport was very low (just above the measurement threshold). At this low current velocity practically no difference in transport was found for waves between $H_s = 0.11$ m and $H_s =$ 0.15m (maximum wave condition which could be reached for the investigated current loading, see below).

$U_{2\%} \ge 0.6 \ m/s \ (i_{2\%}/i_{cr} > 2.3)$

Regular entrainment of sand clouds into filter and water column was observed ($i_{2\%}/i_{cr} = 3.0-4.9$, $u_{2\%}/u_{cr} = 29-45$). A steady increase of base material transport was found for increasing current velocities ($u_{2\%} = 0.6-1.25$ m/s) and increasing wave periods (KC_f numbers).

During the tests it was observed that with increasing current velocity, only a fraction of the generated wave height could be realized (sometimes 50% of generated H_s) in the flume. This is mainly caused by the typical interaction of waves and current (energy conservation: an increase in wave length by stronger currents is followed by a decrease in wave height). In Table 2 only the realized wave heights are given, which correspond to generated wave heights at the wave paddle of $H_s \le 0.2$ m.

Erosion profiles

The measured erosion and filter settlement were very low due to the low amount of base material transport. The measured deviations in filter profile were mainly caused by ripple formation and ripple displacement at the sand-filter interface. The mean profile (averaged over the width of the flume) remained unchanged over all tests (+/- 3mm). Only at local scale (stone diameter size) was erosion and ripple building noticeable up to 1 $D_{n50,f}$ (ca. 20mm). The maximum observed ripple height was approximately equal to the maximum erosion depth. The occurrence of areas of maximum erosion were not correlated to the occurrence of ripple troughs.

TEST RESULTS

In Figures 5 and 6 the measured transport rates are depicted. The lines in the figures show the found trends.

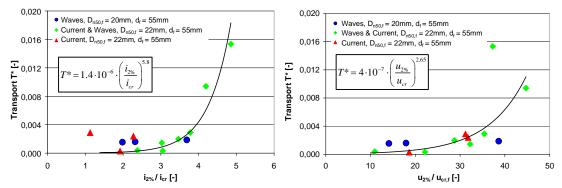


Figure 5. Transport vs. hydraulic gradient and Transport vs. velocity (current, current & wave loading).

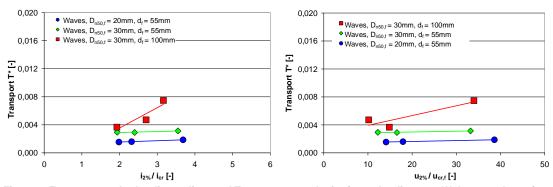


Figure 6. Transport vs. hydraulic gradient and Transport vs. velocity (wave loading, see Wolters et al, 2010).

Figure 5 shows that the measured transport rates (T^*) are strongly correlated to the measured hydraulic gradients $i_{2\%}/i_{cr}$ and velocities $u_{2\%}/u_{cr}$, as already proposed by Klein Breteler *et al* (1992). In contrast to Klein Breteler *et al* (1992) the increase in transport with increasing $i_{2\%}/i_{cr}$ appears to be much stronger (exponent of 5.8 instead of 1.25).

Please note that the filter velocities u_f inside the filter were not actually measured in this study $(u_{2\%})$ is based on the velocities measured 25 mm above the filter), whereas *i* and i_{cr} have been directly measured at the sand-filter interface. The data based on $i_{2\%}/i_{cr}$ are therefore found to be somewhat more reliable.

A strong increase in transport was found for $i_{2\%}/i_{cr} > 3.7$ respectively $u_{2\%}/u_{cr} > 35$. Below these values base material transport was found to be very low (negligible for typical storm durations). Please note also that these gradients ($i_{2\%}/i_{cr} > 3.7$) could not be achieved for the case of wave loading alone (Figure 6).

Recent large scale measurements indicate that under prototype (storm) conditions hydraulic gradients $i_{2\%/i_{cr}}$ of up to 6 can be found (De Vroeg & Muttray, 2009). However, similar gradients could not be generated in the here described small scale tests, indicating that significantly more base material transport can be expected at prototype scale.

Based on the tests on wave loading (Wolters *et al*, 2010), see Figure 6, it was expected that the base material transport would significantly increase for combined current & wave conditions. The stirred up material under wave action, which remained around its rest position and was therefore not transported before, was expected to contribute largely to the measured transport rate. It was also assumed that the transport for current alone was lower than that for combined wave & current action. A strong increase in transport was however not observed for the tested loading cases of current and wave & current. The measured transport rates were still ≤ 0.33 g/m/s (which amounts to about a maximum of 7.5 kg/m per 6 hours) for waves up to H_s =0.15m and currents up to $u_{2\%}$ = 1.2m/s. This indicates a strong 'protective' effect of the tested, relatively thin filter layer ($d_f/D_{n50,f}$ = 1.8-3.3).

Nevertheless, an increase of transport for combined wave & current loading was found (compared to wave loading: factor of up to 7, compared to current loading: factor of up to 5).

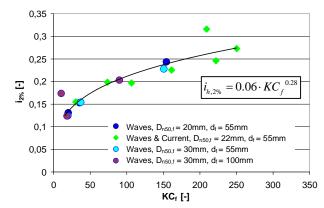


Figure 7. Transport vs. *KC_t* number; *KC_t* is based on the velocity measured 25mm above the filter bed, $u_{2\%}$, and the filter thickness d_t (*KC_t* = $u_{2\%}T_m/[n_td_t]$)

Figure 7 shows that a strong relationship was found between KC_f number and hydraulic gradient $i_{2\%}$. The figure (in combination with Figure 5) indicates that base material transport can be described as a function of i/i_{cr} ($T = f(i/i_{cr})$), where the hydraulic gradient *i* is given as a function of KC_f . However, the indicated trends (relationships) need further verification, especially regarding the possible influence of variations in filter thickness. Filter thickness was expected to have an influence on the hydraulic gradient, although for the tested two filter thicknesses no influence could be found.

Influence of filter

In Test T13 (current alone) and Test T14 (current & waves) the filter layer ($d_f/D_{n50,f} = 2.5$) was completely removed to acquire reference data on the material transport without filter. A strong effect on bed material transport was observed:

For current loading, the transport increased from 0.006 g/m/s to 12.3 g/m/s (factor 2050) and for combined wave & current loading from 0.043 g/m/s to 33.6 g/m/s (factor 781), see Figure 8 (left). Because of the large quantities of sand transported, each test was stopped after 30 minutes.

Without the protection of the filter layer, the entire top layer of the sand bed came into motion when waves passed over it (whereas only localized particle motion was observed for the current-alone test T13). In contrast to the tests with filter, the bedforms of the sand changed also: much larger variances in size and form of ripples (ripples with steep rearside and symmetric ripples of half-circle form) were observed.

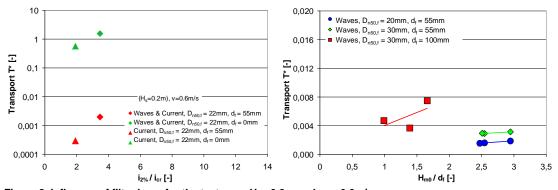


Figure 8. Influence of filter layer for the test case $H_s = 0.2m$ and $u_m = 0.6m/s$.

Figure 8 (right) indicates that varying filter thickness affects the sand transport rates more strongly than varying filter material diameters (only investigated for wave loading case). As indicated before, the effect of filter thickness needs further research, since the present data is insufficient. Please note that the measured transport rates for the case of $d_f = 0.1$ m are larger than for a filter thickness of $d_f = 0.055$ m. This finding appears counterintuitive and cannot be explained at present.

Comparison with macroscopic transport model of Klein Breteler et al (1992)

If the results of the present investigation are compared with the (steady flow) model of Klein Breteler *et al* (1992), it becomes apparent that the predicted transport rates based on Equation 5 are much larger than measured in the present tests (by factor of 30 - 920). On the other hand, the increase in transport with increasing i/i_{cr} is significantly lower $((i/i_{cr})^{1.25}$ compared to $(i/i_{cr})^{5.8}$ in the present tests). This large deviation is found for all loading cases (current, wave, wave & current). At present it is assumed that the main reason for the deviations is the varying model set-up: Klein Breteler *et al* (1992) used a closed 'filter box', which guaranteed a nearly constant filter velocity over the depth, while the present tests were conducted with a free water surface. Also note that Klein Breteler *et al*'s (1992) study investigated current loading and included no waves.

CONCLUSIONS

The presented 2D physical model study focussed on geometrically open granular filters on a submerged, horizontal sand bed. Tests were conducted for filters under wave, current and combined wave & current loading. The following conclusions were drawn:

- Bed material (sand) transport in a granular filter structure can be described as function of the hydraulic gradient $i_{2\%}/i_{cr}$, independent of the loading condition (wave / current / wave & current).
- The hydraulic gradient $i_{2\%}/i_{cr}$ can be estimated using the modified Keulegan-Carpenter (KC_f) number.
- For hydraulic gradients $i_{2\%/i_{cr}} < 3$, a thin protective granular filter layer $(d_f = 2D_{n50,f} 3D_{n50,f})$ on top of the sand bed was observed to reduce the sand transport rates so far that no significant bed erosion (damage) occurred.
- For conditions with a current alone and conditions with waves only, very low base material transport rates were recorded (<0.06 g/m/s respectively <0.16 g/m/s). For conditions with a combination of waves and a current the transport increased somewhat (up to 0.33 g/m/s) for generated waves up to H_s =0.2m and depth-averaged current velocities of u_m =1m/s.
- A strong increase in transport was found for hydraulic gradients $i_{2\%}/i_{cr} > 3.7$ (storm conditions). For these conditions significant erosion of the base material is expected in prototype. Recent large scale measurements indicate that under prototype (storm) conditions hydraulic gradients $i_{2\%}/i_{cr}$ of up to 6 can be found (De Vroeg & Muttray, 2009).
- A dominant effect of filter thickness on base material transport was found. Due to the limited amount of performed tests, this effect needs further study. The same is valid for the influence of filter gradation and bed slope, which were not investigated in this study.
- An equilibrium situation (after initial scouring) has so far not been found in any of the conducted studies.
- Verification of the results at large model scale and under oblique waves is recommended.

REFERENCES

Bakker K.J., Verheij H.J., and de Groot M.B. 1994. Design relationship for filters in bed protection". J. Hydraulic Eng., 120(9), 1082-1088.

CUR report 161. 1993. Filters in hydraulic engineering, Gouda (in Dutch).

- CUR report 233. 2010. Interface stability of granular filter structures, Theoretical design methods for currents, CURNET, Gouda.
- Den Adel H. 1992. Transport model for filters, Deel 1-3, report C0-325970/6, Delft Hydraulics (in Dutch).
- De Graauw, A., Van der Meulen, T., Van der Does de Bye, M. 1983. Design criteria for granular filters, Publication 287, Delft Hydraulics.
- Dixen, F.H., Sumer, B.M. and Fredsoe, J. 2008. Suction removal of sediment from between armor blocks. II: waves, J. of Hydraul. Eng., Vol 134, no 10, October 2008, ASCE.
- Klein Breteler M. 1989. Sand transport in granular filters, horizontal steady current, report H869, Delft Hydraulics (in Dutch).
- Klein Breteler M., Den Adel H., Koenders M.A. 1992. Slope protections of set stone (revetment), Design rules for the filter layer, Report M1795/H195, XXI, Delft Hydraulics & Geo Delft (in Dutch).
- Ockeloen, W.J. 2007. Open filters in breakwaters with a sand core, M.Sc. thesis, TU Delft.

- Sumer, B. M., Cokgor, S., and Fredsøe, J. 2001. Suction removal of sediment from between armor blocks, J. Hydraul. Eng., 127(4), 293–306.
- Uelman, E.F. 2006. Geometrically open filters in breakwaters, M.Sc. thesis, TU Delft.
- Van Gent, M.R.A. 1995. Wave interaction with permeable coastal structures, Ph.D.-dissertation, Delft University of Technology, ISBN 90-407-1182-8, Delft University Press, Delft.
- Vroeg de J.H. and Muttray M. 2009. Stability of sand under an open filter, Desk study, Deltares, internal communication (in Dutch).
- Wolters G., D. Rudolph, B. Hofland, H. Verheij. 2010. On the behaviour of Open Filters under wave loading, Proc. 5th International Conference on Scour and Erosion (San Francisco), Geotechnical Special Publication 210, ASCE.